Biochemical and Biophysical Research Communications 443 (2014) 511–517

Contents lists available at ScienceDirect

Biochemical and Biophysical Research Communications

journal homepage: www.elsevier.com/locate/ybbrc

N′-[4-(dipropylamino)benzylidene]-2-hydroxybenzohydrazide is a dynamin GTPase inhibitor that suppresses cancer cell migration and invasion by inhibiting actin polymerization

Hiroshi Yamada [a,e,*,1], Tadashi Abe [a,e,1], Shun-Ai Li [b], Shota Tago [a], Peng Huang [b], Masami Watanabe [b], Satoru Ikeda [c], Naohisa Ogo [d], Akira Asai [d], Kohji Takei [a,e]

[a] Department of Neuroscience, Okayama University, Graduate School of Medicine, Dentistry and Pharmaceutical Sciences, 2-5-1, Shikata-Cho, Kita-ku, Okayama 700-8558, Japan
[b] Department of Urology, Okayama University, Graduate School of Medicine, Dentistry and Pharmaceutical Sciences, 2-5-1, Shikata-Cho, Kita-ku, Okayama 700-8558, Japan
[c] Department of Medical Technology, Graduate School of Health Sciences, Okayama University, 2-5-1, Shikata-Cho, Kita-ku, Okayama 700-8558, Japan
[d] Center for Drug Discovery, Graduate School of Pharmaceutical Sciences, University of Shizuoka, 52-1, Yada, Suruga-ku, Shizuoka 422-8526, Japan
[e] CREST, JST, 2-5-1, Shikata-Cho, Kita-ku, Okayama 700-8558, Japan

ARTICLE INFO

Article history:
Received 16 November 2013
Available online 6 December 2013

Keywords:
Dynasore
Dynamin
Actin cytoskeleton
Migration
Invasion
GTPase

ABSTRACT

Dynasore, a specific dynamin GTPase inhibitor, suppresses lamellipodia formation and cancer cell invasion by destabilizing actin filaments. In search for novel dynamin inhibitors that suppress actin dynamics more efficiently, dynasore analogues were screened. N′-[4-(dipropylamino)benzylidene]-2-hydroxybenzohydrazide (DBHA) markedly reduced in vitro actin polymerization, and dose-dependently inhibited phosphatidylserine-stimulated dynamin GTPase activity. DBHA significantly suppressed both the recruitment of dynamin 2 to the leading edge in U2OS cells and ruffle formation in H1299 cells. Furthermore, DBHA suppressed both the migration and invasion of H1299 cells by approximately 70%. Furthermore, intratumoral DBHA delivery significantly repressed tumor growth. DBHA was much less cytotoxic than dynasore. These results strongly suggest that DBHA inhibits dynamin-dependent actin polymerization by altering the interactions between dynamin and lipid membranes. DBHA and its derivative may be potential candidates for potent anti-cancer drugs.

1. Introduction

Cancer cell migration and invasion are led by pseudopodia, plasma membrane protrusions generated by the dynamic remodeling of actin. Since actin dynamics are regulated by several cytosolic proteins [1], small molecule inhibitors targeting these actin-regulating proteins may have therapeutic anti-cancer activity.

Dynamin, a fission protein involved in clathrin-mediated endocytosis [2–4], has been implicated in the formation of actin-rich structures, including lamellipodia and dorsal membrane ruffles [5–6], invadopodia [7], podosomes [8], growth cones [9,10], and phagocytic cups [11,12]. Dynamins are composed of three isoforms, dynamin 1–3 [4], which share a common domain structure. Dynamin includes a GTPase domain at N-terminus, a bundle signaling element (BSE), a stalk domain, and a domain with phosphoinositide-binding pleckstrin homology (PH) and C-terminus of dynamin contains proline/arginine-rich domain (PRD) [13,14]. The PRD interacts with various proteins that contain SH3 domain.

Dynamin GTPase activity is crucial for actin regulation. Expression of the dynamin GTPase-defective mutant, K44A, in HeLa cells alters the arrangement of stress fibers [15]. Actin filaments formed in vitro are remodeled upon dynamin-mediated hydrolysis of GTP [16,17]. More recently, we found that dynamin and cortactin polymerize to form a ring-shaped complex, which mechanically bundles actin filaments by undergoing an open-and-closed motion upon GTP hydrolysis [10].

Several inhibitors of dynamin GTPase have been used to analyze dynamin-dependent endocytosis [18]. One of these, dynasore, a non-competitive inhibitor [19], destabilizes actin filaments and inhibits cell migration and invasion [20]. These results suggest that inhibitors of dynamin GTPase could be potential candidates for anti-cancer drugs. Therefore, we screened novel dynamin inhibitors to identify those that inhibited cancer cell migration and invasion. To this end, we developed an in vitro actin polymerization assay, and assayed dynasore analogues. We found that DBHA inhibited ruffle formation and cancer cell migration and invasion.

2. Materials and methods

2.1. Reagents and antibodies

Dynasore was purchased form Sigma–Aldrich (St. Louis, MO). DBHA was from Vitas-M Lab Ltd. (Moscow, Russia). Polyclonal goat

* Corresponding author. Fax: +81 86 235 7126.
E-mail address: hiroyama@md.okayama-u.ac.jp (H. Yamada).
[1] The first two authors equally contributed to the work.

0006-291X/$ - see front matter © 2013 Elsevier Inc. All rights reserved.
http://dx.doi.org/10.1016/j.bbrc.2013.11.118

anti-dynamin 2 antibody (sc-6400) was from Santa Cruz Biotechnology (Santa Cruz, CA), mouse monoclonal antibody against cortactin (05-180) was from Millipore (Billerica, MA).

2.2. Animals

Ten-week-old C57BL/6J male mice were purchased from Shimizu Laboratory Supplies Co. (Kyoto, Japan). Mice were maintained in a specific pathogen-free environment at the laboratory animal center of Okayama University, and had free access to food and water in accordance with the Okayama University Animal Research Committee Guidelines.

2.3. Cell culture

H1299 (ATCC No; CRL-5803), U2OS (ATCC No; HTB96), and PC3 (ATCC No; CRL-1435) cells were cultured in Dulbecco's modified Eagle's medium (DMEM; Life Technologies Corp., CA) supplemented with 10% fetal bovine serum (FBS; Life Technologies Corp., CA) at 37 °C in humidified air with a 5% CO_2 atmosphere.

2.4. Immunocytochemistry and ruffle formation

U2OS cells (1×10^4 cells/coverslip) were starved in 0.2% FBS/DMEM for more than 16 h, and treated with 10% FBS/DMEM for 40 min, fixed with 4% paraformaldehyde in phosphate buffered saline (PBS), permeabilized with 0.1% Triton-X100, and double stained by immunofluorescence as described [20].

To induce ruffle formation, serum-starved H1299 cells were pre-incubated with inhibitors at the indicated concentrations for 30 min, then stimulated with 10% FBS/DMEM for 10 min at 37 °C in the presence of inhibitors. As a negative control, cells were treated with 1% DMSO. To remove DBHA, the cells were quickly washed twice with PBS, incubated with 0.2% FBS/DMEM for 30 min, and stimulated with 10% FBS/DMEM for 10 min. Cells showing F-actin-rich membrane extensions were defined as ruffle-positive cells [21]. To assess ruffle formation, cells were labeled with rhodamine-phalloidin, and analyzed by fluorescent confocal microscopy as described above.

2.5. In vitro actin assay

F-actin formation was quantitatively analyzed using pyrene-actin as described [10,22]. For the visual assays, 1 μM rhodamine-actin (Life Technologies Corp., CA) was added to 20 mg/ml of mouse brain cytosol and F-actin formation was induced by the addition of 120 μM liposomes composed of 50% Phosphatidylserine and 50% Phosphatidylcholine. To examine the effects of the inhibitors, brain cytosol was pre-incubated with 80 μM dynasore or DBHA for 10 min, or with 10 μM cytochalasin D for 5 min; liposomes were then added and the mixture were incubated for 40 min at room temperature. F-actin formation was assayed by fluorescent confocal microscopy.

2.6. Wound healing assay

H1299 cells were plated to confluence on glass-bottom dishes (35 mm diameter; IWAKI Glass Co. Ltd.), cultured in 0.2% FBS/DMEM for 16 h and then wounded with a plastic pipette tip as previously described [23]. After washing with 0.2% FBS/DMEM, the cells were incubated for 8 h with 0.2% FBS/DMEM supplemented with dynasore or DBHA at the indicated concentrations. As a negative control, cells were incubated with 1% DMSO. The cells were visualized by Giemsa staining, followed by the acquisition of phase contrast images from at least 20 different areas randomly selected area per dish. Areas filled by cell migration were determined by analyzing the resulting images using Image J software.

2.7. Cell invasion assay

Invasion assays were performed in 24-well Matrigel invasion chambers with 8 μm pores (BD Biosciences, Bedford, MA) as described [24]. H1299 cells (2.5×10^5 cells/well) were seeded in the upper chamber in serum-free DMEM and DMEM containing 50% FBS was placed in the bottom chamber. After 8 h, DBHA or dynasore was added to both the upper and lower chambers and the cells were incubated for a further 8 h. Cells on the upper side of the membrane were scraped off, whereas cells on the bottom of each membrane were fixed in methanol and stained with toluidine blue. Invasive cells were counted on micrographs of a total of 15 fields (five fields from each of three independent experiments) taken at ×200 magnification.

2.8. Dynamin GTPase assay

GTP hydrolysis was measured at 1 mM GTP using a colorimetric assay to detect Pi release as previously described [25]. His-tagged dynamin 1 was expressed using the Bac-to-Bac baculovirus expression system (Life Technologies) and purified as described [10].

2.9. In vivo anti-tumor assay

Human prostate cancer PC3 cells (5×10^6 cells) were subcutaneously injected into the right thigh of male athymic [nu/nu] mice (6–7 weeks-old) from CLEA Japan, Inc. (Tokyo, Japan). The subcutaneous tumors were allowed to reach 7–13 mm in size and the mice were randomized into 3 groups of five animals each. Next, the mice were intratumorally treated with the dynasore (0.5 mg/mouse) or DBHA (0.5 mg/mouse) in 100 μl of vehicle (5% DMSO in PBS). As a negative control, the same volume of vehicle was used. The injections were targeted to the center and periphery of the tumor to deliver the agent diffusely. The size of the tumors was measured at the indicated day points and tumor volume was calculated using the formula, $1/2 \times (\text{the longest diameter}) \times (\text{the shortest diameter})^2$ [24].

2.10. Statistical analysis

DATA were analyzed using KaleidaGraph (v 4.1) for Macintosh (Synergy Software) to perform statistical analysis. ANOVA and Tukey's HSD *post hoc* test were applied.

3. Results

3.1. DBHA inhibits both in vitro actin polymerization and dynamin GTPase activity

We previously demonstrated that dynasore, a specific inhibitor of dynamin GTPase, suppresses cancer cell migration and invasion and destabilizes actin filaments [20]. To identify more effective dynamin inhibitors, dynasore analogues, each at a concentration of 40 μM, were screened in an in vitro actin polymerization assay with pyrene-conjugated actin [10,21,22] (Fig. 1A and B). Among the tested compounds, N′-[4-(dipropylamino)benzylidene]-2-hydroxybenzohydrazide (DBHA) (Fig. 1C) showed the greatest inhibitory effect on F-actin formation. Treatment of brain cytosol with DBHA inhibited F-actin formation in a dose-dependent manner, with ~85% inhibition at 40 μM (Fig. 1B, D and E). IC_{50} values were 7 μM for DBHA and 18 μM for dynasore (Fig. 1E). Morphological analysis consistently demonstrated that treatment of brain

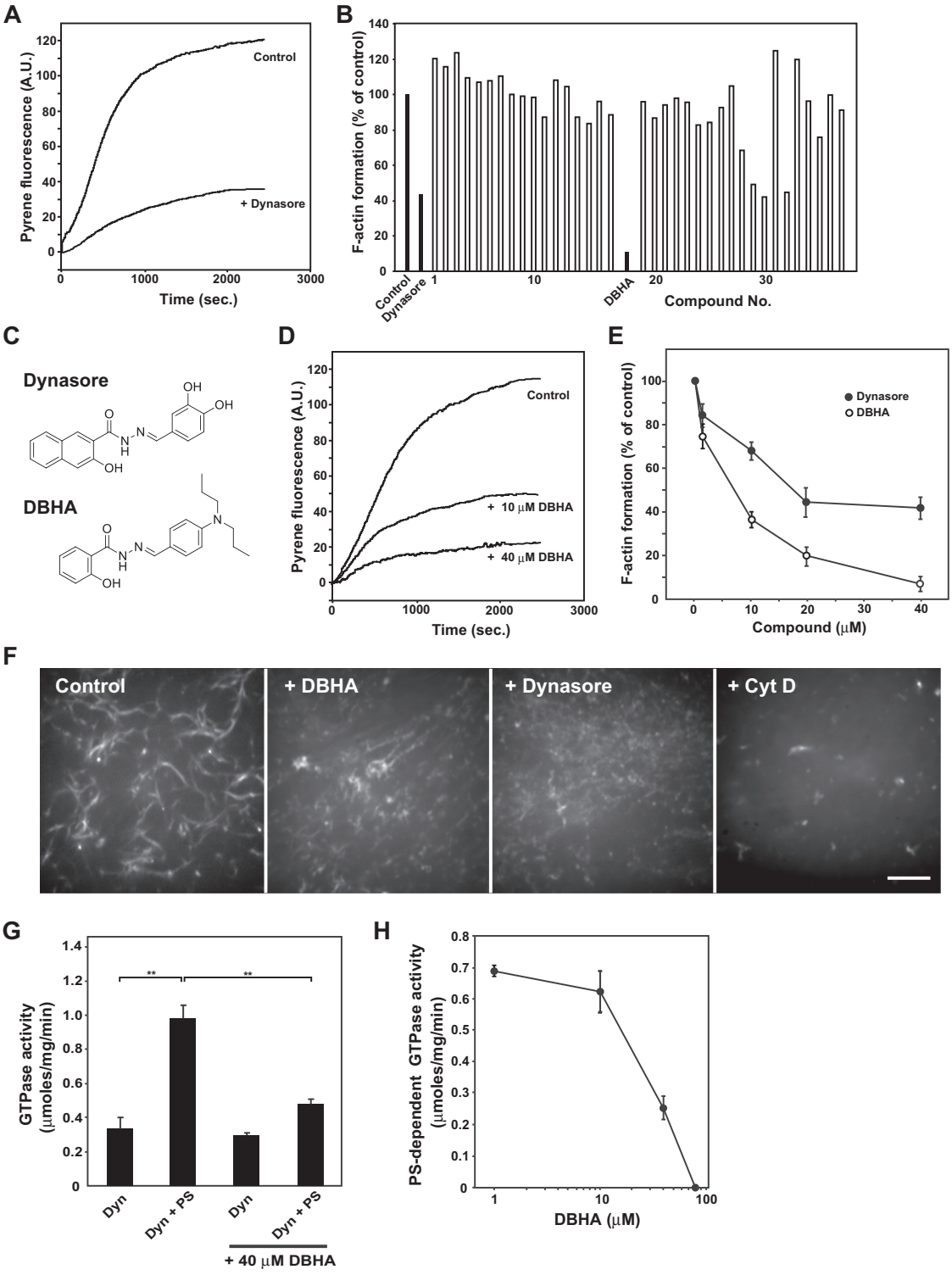

Fig. 1. DBHA strongly inhibits PS-induced actin polymerization in vitro. (A) Typical time-course of pyrene fluorescence caused by in vitro actin polymerization. Mouse brain cytosol was treated with PS-containing liposomes in the presence of 40 μM dynasore, or, as a control, 1% DMSO. The time 0 indicates the time at which the liposomes were added. (B) Actin polymerization activity in brain cytosol treated with several dynasore analogues, each at concentration of 40 μM. Pyrene fluorescence was measured at 2000 s. Dynasore analogues were tested and some of the results were shown. All activities were normalized relative to control brain cytosol incubated with 1% DMSO. (C) Chemical structures of dynasore and DBHA (D) Time-course of pyrene fluorescence during in vitro actin polymerization with increasing concentrations of DBHA. (E) Dose-dependent inhibition of actin polymerization by dynasore or DBHA. F-actin formation was measured at 2000 s in the presence of increasing concentrations of dynasore or DBHA. (F) In vitro actin polymerization visualized with rhodamine-actin. Actin filaments and bundles were evident in the negative controls, not observed formed F-actin in the presence of Cytochalasin D (Cyt D), an inhibitor for actin polymerization. In the presence of DBHA or dynasore, the formation of actin filaments and actin bundles was decreased. Bar: 10 μm. (G) Effect of DBHA on basal and PS-dependent dynamin GTPase activity. Dynamin 1 (50 nM) was pre-incubated with DBHA (40 μM) for 20 min, and then stimulated with 15 μM PS-containing liposomes. The graph is representative of three independent experiments. All results represent the mean ± S.E.M. (**: $p < 0.001$). (H) PS-dependent GTPase activity of dynamin 1 (50 nM) determined in the presence of increasing concentrations of DBHA. The graph is representative of three independent experiments.

cytosol with either DBHA or dynasore significantly reduced the numbers of long and thick actin filaments and the bundles induced by phosphatidylserine (PS) in vitro (Fig. 1F).

Next, we examined the effect of DBHA on dynamin GTPase activity. Binding of the dynamin PH domain to PS or PtdIns(4,5)P_2 increases the GTPase activity of dynamin [26,27]. DBHA dose-dependently inhibited PS-dependent dynamin GTPase activity, with an IC_{50} for DBHA of 26 μM (Fig. 1G and H). Under our experimental conditions, dynasore at 80 μM inhibited PS-dependent GTPase activity by 26.7 ± 3.1% (n = 3), suggesting that DBHA is a more potent dynamin GTPase inhibitor.

3.2. DBHA decreases accumulation of dynamin 2 on the leading edge of plasma membranes

Dynamin is recruited to actin-enriched pseudopodia, including leading edges and ruffles [6]. This recruitment is mediated by the interaction between the dynamin PH domain and the phosphoinositides in the plasma membrane [12,28]. To determine whether DBHA could cause dynamin dysfunction in vivo, the recruitment of dynamin 2 to pseudopodia in plasma membranes was investigated in a osteocarcinoma cell line, U2OS. Upon serum stimulation, U2OS cells formed large numbers of pseudopodia, and both dynamin 2 and cortactin, a marker for membrane ruffles [6], accumulated at the leading edge (Fig. 2A a–c). Treatment with DBHA prior to serum stimulation markedly reduced the recruitment of dynamin 2 to the leading edge (Fig. 2A d–f). Removal of DBHA followed by re-stimulation with serum, again resulted in the recruitment of dynamin 2 to the leading edge, suggesting that the effects of DBHA are reversible (Fig. 2A g–i). The inhibitory effect of DBHA on cells was similar to that of dynasore (Fig. 2A j–o).

3.3. DBHA decreases both migration and invasion of lung cancer cells

Since dynamin is required for ruffle formation, cancer cell migration and invasion [20,23,29], we next examined whether DBHA inhibits these cellular activities. H1299 cells, a human lung cancer cell line, were incubated with various concentrations of DBHA or dynasore and cells showing ruffle formation were assessed. Actin-rich ruffle formation was dose-dependently inhibited by DBHA with ~85% inhibition at 40 μM (Fig. 3A and B), but reappeared after washing out DBHA (Fig. 3B). Furthermore, a wound healing assay showed that DBHA dose-dependently suppressed the migration of H1299 cells with ~70% inhibition at 40 μM (Fig. 3C and D). The effect of DBHA on H1299 invasiveness was then examined in a Matrigel invasion chamber. In the absence of DBHA, a significant number of H1299 cells were attracted to the high (50%) concentration of FBS, and invaded through the membrane of the chamber (Fig. 3E and F). However, H1299 invasiveness was dose-dependently inhibited by DBHA, with ~70% inhibition at 40 μM (Fig. 3E and F).

Next, anti-tumor activity of DBHA was examined in vivo. Tumors of PC3 were formed subcutaneously in mice, and DBHA or dynasore were injected intratumorally. Four days after the treatments, significant inhibition of tumor growth was observed in the mice treated with dynasore and DBHA in comparison to control treatment with vehicle (5% DMSO/PBS) (Fig. 3G). Eight days after the treatments, the anti-tumor effect was significantly potent in the DBHA treated mice in comparison to the other groups. At the necropsy, we also examined the toxic effects in the three treatment groups and there was no apparent adverse effect in the groups.

Finally, the cytotoxicity of DBHA and dynasore was determined. Incubation of H1299 cells with 50 μM dynasore reduced cell viability by 50% after for 72 h, whereas incubation with 50 μM DBHA reduced viability by only 15%. The low level of cytotoxicity

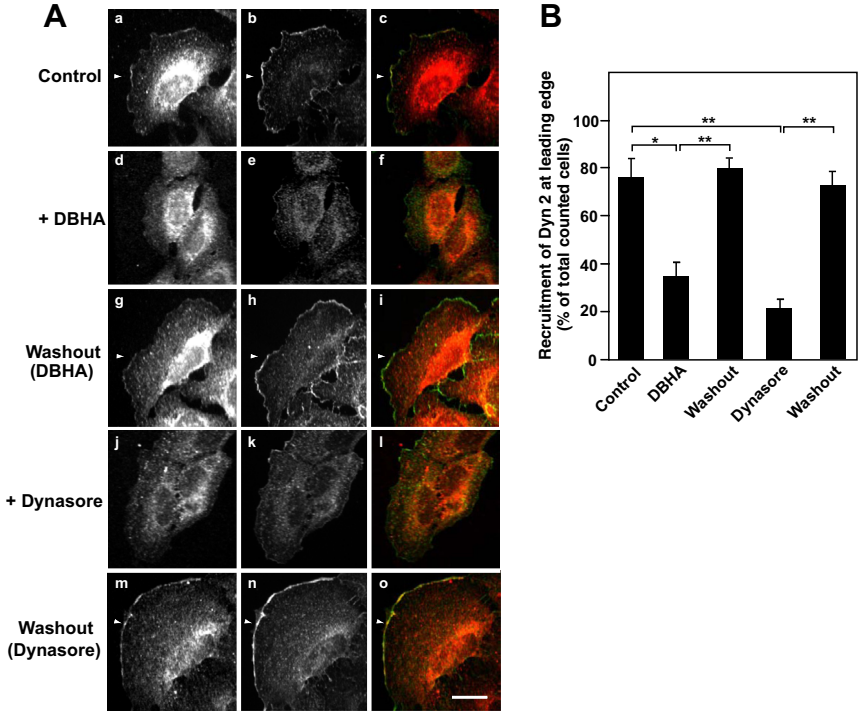

Fig. 2. DBHA prevents the recruitment of dynamin 2 to the leading edge of U2OS cells. (A) Serum-starved U2OS cells were pre-treated with 80 μM DBHA or dynasore for 30 min and stimulated with 10% FBS/DMEM for 40 min in the presence of DBHA (d–f) or dynasore (j–l). Control cells were treated with 1% DMSO (a–c). For the "Washout" samples, cells treated with DBHA (g–i) or dynasore (m–o) as above were washed twice with PBS and re-stimulated with 10% FBS/DMEM for 40 min. After the incubations, the cells were fixed, permeabilized, and double-stained by immunofluorescence for dynamin 2 (a, d, g, j, and m) and cortactin (b, e, h, k, and n). The merged images are shown in the right column. Bar: 20 μm. Arrowheads indicate leading edges. Note the absence of dynamin 2 at the leading edge of DBHA or dynasore-treated cells (d, j). (B) Morphometric analysis of the recruitment of dynamin 2 to the leading edge. (*: $p < 0.005$, **: $p < 0.001$).

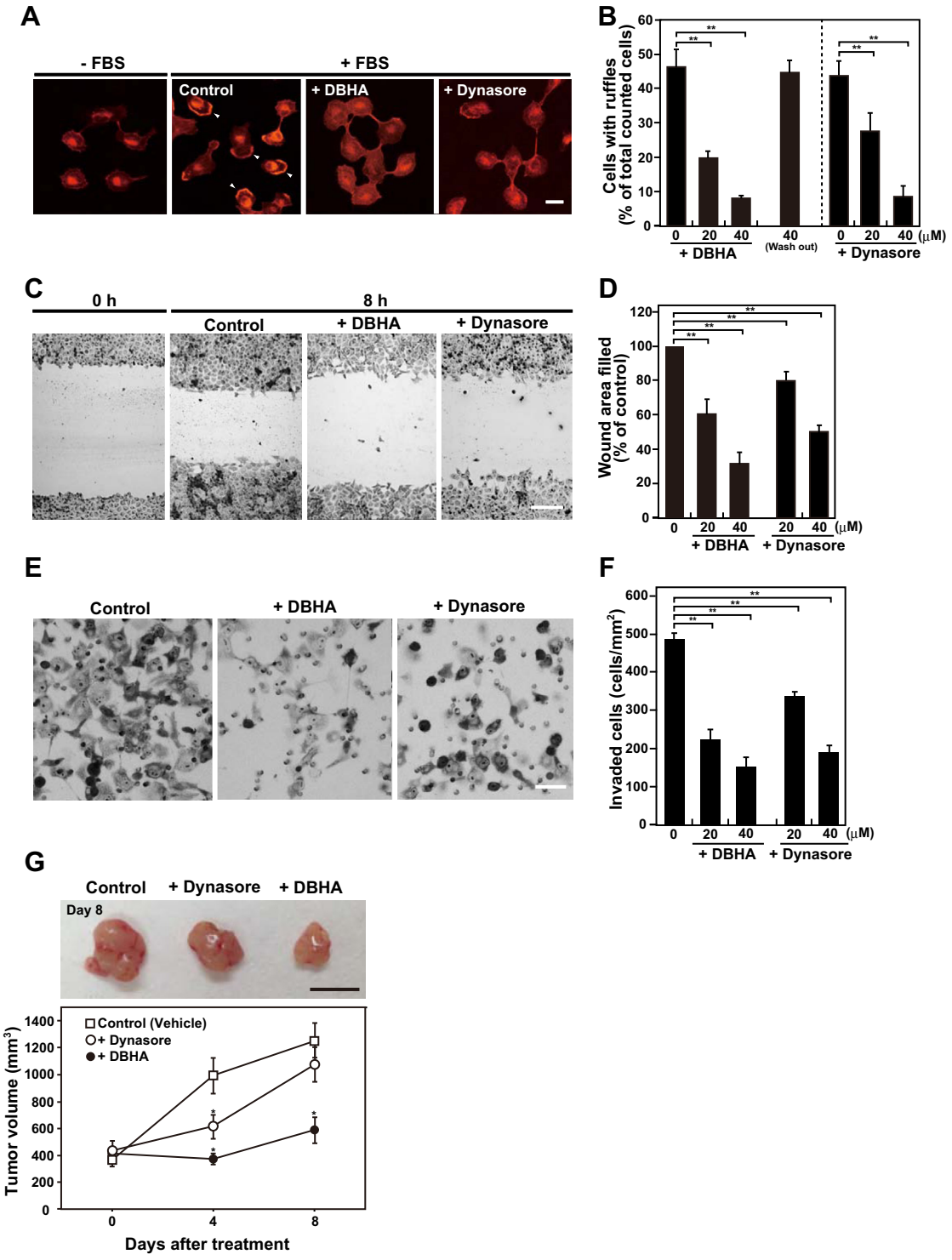

Fig. 3. DBHA inhibits ruffle formation, cell migration, and invasion by H1299 cells. (A) Ruffle formation by H1299 cells in the presence or absence of 40 μM DBHA or dynasore. Serum-stimulated cells were fixed and labeled with rhodamine-phalloidin. While many ruffles were observed in the control cells (arrowheads), DBHA or dynasore inhibited the ruffle formation. Bar: 20 μm. (B) Morphometric analysis of ruffle formation in A. More than 50 cells were counted in 10 independent fields. All results represent the mean ± S.E.M. of the three independent experiments. (**: $p < 0.001$). (C) Light microscopy showing cell migration in a wound healing assay. Confluent cultured H1299 cells were wounded and incubated for 8 h in the presence or absence of 40 μM DBHA or dynasore. Bar: 100 μm. (D) Morphometric analysis of the wound area filled by migrating cells in the presence of DBHA or dynasore at the indicated concentrations. All activities are normalized to the filled area of the control. All results represent the mean ± S.E.M. of the three independent experiments. (**: $p < 0.001$). (E) In vitro invasion assay using a Matrigel invasion chamber. Representative images of invasive cells in the presence or absence of 40 μM DBHA or dynasore. Cells were stained with toluidine blue. Bar: 20 μm. (F) Morphometric analysis of the invasive cells in E. Results are expressed as the mean ± S.E.M. of three independent experiments. (**: $p < 0.001$). (G) Suppression of tumor growth by intratumoral DBHA delivery. Representative image of PC3 tumors on day 8 after DBHA, dynasore or vehicle treatment (Upper panel). Tumor sizes were measured at day 0, day 4 and day 8, and the calculated volumes were shown in the lower panel. Bar: 1 cm. Results are expressed as the mean ± S.E.M. (*: $p < 0.05$).

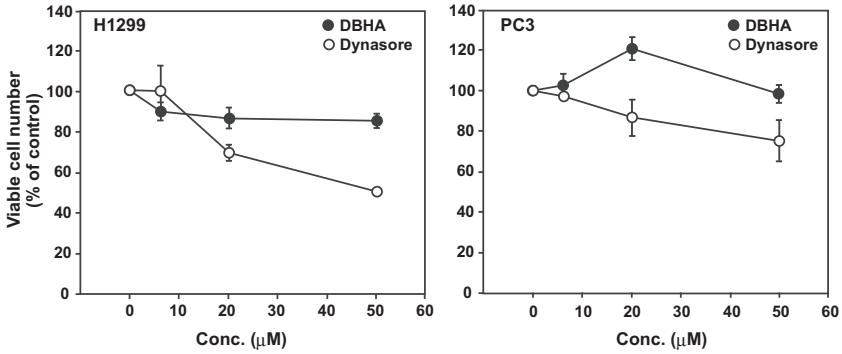

Fig. 4. DBHA is less cytotoxic to H1299 and PC3 cells than dynasore. Two cancer cell lines, H1299 (left) and PC3 (right), were exposed to increasing concentrations of DBHA or dynasore for 72 h. Cell viability was determined with the cell proliferation reagent WST-1 kit (Roche Applied Science, Mannheim, Germany) as described by the manufacturer. All results are expressed as the mean ± S.E.M. of the three independent experiments.

mediated by DBHA was confirmed in PC3 cells, a human prostate prostatic adenocarcinoma cell line. Incubating these cells with 50 μM DBHA for 72 h had no effect on cell viability, whereas incubation with 50 μM dynasore reduced viability to 75% (Fig. 4). Thus, DBHA was much less cytotoxic than dynasore under these experimental conditions.

4. Discussion

Dynasore, a dynamin inhibitor, suppresses lamellipodia formation and cancer cell invasion by destabilizing actin filaments, suggesting its potential as an anti-cancer drug [20]. To identify more potent compounds, we screened dynasore analogues for their ability to inhibit actin polymerization in vitro. We found that DBHA not only inhibited in vitro actin polymerization but also PS-stimulated dynamin GTPase activity (Fig. 1). Thus, DBHA-mediated inhibition of dynamin GTPase likely resulted in reduced actin polymerization.

Accumulating evidence indicates that dynamin is a direct or indirect regulator of actin filaments. Dynamin is required for the formation of actin-based structures such as lamellipodia, ruffles, and phagocytic cups [6–12]. Dynamin interacts not only with a variety of actin-regulating proteins such as cortactin, α-actinin 4, profilin and Abp1 [6,30–32], but also directly with actin filaments [33].

Dynamin GTPase activity appears to be essential for its regulation of actin Incubation of actin filaments with dynamin and cortactin in vitro resulted in the formation of tight actin bundles [10,17]. These actin bundles cross-linked with nucleotide-free dynamin 2 and cortactin, with apparent changes in morphology upon the addition of GTP [17]. In addition, actin bundles formed in vitro with dynamin 1/cortactin complexes are more stable in the presence of GTP than GDP, or under nucleotide-free conditions [10]. Moreover, dynamin GTPase activity is likely involved in regulating the actin cytoskeleton in cells. Stress fiber rearrangements have been observed in fibroblasts that express dynamin K44A, a GTPase deficient mutant [15]. Moreover, expression of dynamin K44A in MDCK epithelial cells resulted in increased apical constriction [34].

The presence of the lipid membrane potentiates actin polymerization. During in vitro actin polymerization, PS- or phosphoinositide-containing liposomes provide scaffolds for the recruitment of actin-binding proteins, including dynamin, which in turn stimulate actin polymerization on liposomes. Dynasore consistently inhibits liposome-stimulated actin polymerization [12]. In cells, the recruitment of dynamin to the plasma membrane is essential for the formation of actin-rich structures [6,12]. DBHA decreased the recruitment of dynamin 2 to the plasma membrane (Fig. 2), which may, in turn, have decreased dynamin GTPase activity and dynamin-stimulated actin polymerization.

Dynamin was recently found to be associated with tumor malignancy, particularly tumor cell migration and invasion. For example, up-regulation of dynamin 2 expression potentiates migration and invasion in pancreatic ductal carcinomas [23], and tyrosine phosphorylated dynamin 2 enhances the growth and invasiveness of glioblastomas [29]. Accordingly, dynamin is now regarded as a potential molecular target for anti-cancer therapeutics. We found that DBHA inhibited both cancer cell migration and invasion (Fig. 3), likely by inhibiting dynamin-stimulated actin polymerization. Furthermore, DBHA suppressed tumor more potently in comparison to dynasore in the human prostate cancer mouse model with no apparent adverse effect (Fig. 3G).

Although DBHA and dynasore showed similar inhibitory activities, DBHA was much less cytotoxic than dynasore in cells (Fig. 4). In addition to DBHA and dynasore, a series of myristoil trimethyl ammonium bromides (MiTMABs) were identified as potent dynamin inhibitors based on their inhibition of dynamin GTPase activity [28]. MiTMABs cause cytokinesis failure and strongly inhibit the proliferation of cancer cells [35]. These results are thought to be due to the effect of dynamin on cytokinesis [36].

In conclusion, we identified a new dynamin inhibitor, DBHA, which strongly blocked the migration and invasion of cancer cells by inhibiting dynamin-stimulated actin polymerization, but showed low cytotoxicity. Most of molecular targets of current anti-cancer drugs are involved in the processes of cell division or DNA replication. Therefore, DBHA may be a leading compound for an anti-cancer drug that has a novel mechanism of action; targeted for dynamin-dependent actin dynamics. Further studies are needed to determine the precise mechanism (s) by which DBHA inhibits actin dynamics.

Acknowledgments

This work was supported by a Grant-in-Aid for Scientific Research from the Ministry of Education, Science, Sports and Culture of Japan to K.T. (23370089), by Astellas Foundation for Research on Metabolic Disorders to H.Y., by Intractable Infectious Diseases Research Project Okayama to H.Y. and by the Japan Foundation for Applied Enzymology to H.Y. We thank Miss Mikako Arita, Miss Nana Okazaki, Miss Mami Danjyo, and Mr. Tadahiko Inoue for technical assistance.

References

[1] T.D. Pollard, G.G. Borisy, Cellular motility driven by assembly and disassembly of actin filaments, Cell 112 (2003) 453–465.

[2] K. Takei, V.I. Slepnev, V. Haucke, et al., Functional partnership between amphiphysin and dynamin in clathrin-mediated endocytosis, Nat. Cell Biol. 1 (1999) 33–39.
[3] M. Mettlen, T. Pucadyil, R. Ramachandran, et al., Dissecting dynamin's role in clathrin-mediated endocytosis, Biochem. Soc. Trans. 37 (2009) 1022–1026.
[4] G.J. Praefcke, H.T. McMahon, The dynamin superfamily: universal membrane tubulation and fission molecules?, Nat Rev. Mol. Cell Biol. 5 (2004) 133–147.
[5] H. Cao, F. Garcia, M.A. McNiven, Differential distribution of dynamin isoforms in mammalian cells, Mol. Biol. Cell 9 (1998) 2595–2609.
[6] M.A. McNiven, L. Kim, E.W. Krueger, et al., Regulated interactions between dynamin and the actin-binding protein cortactin modulate cell shape, J. Cell Biol. 151 (2000) 187–198.
[7] M. Baldassarre, A. Pompeo, G. Beznoussenko, et al., Dynamin participates in focal extracellular matrix degradation by invasive cells, Mol. Biol. Cell 14 (2003) 1074–1084.
[8] G.C. Ochoa, V.I. Slepnev, L. Neff, et al., A functional link between dynamin and the actin cytoskeleton at podosomes, J. Cell Biol. 150 (2000) 377–389.
[9] E. Torre, M.A. McNiven, R. Urrutia, Dynamin 1 antisense oligonucleotide treatment prevents neurite formation in cultured hippocampal neurons, J. Biol. Chem. 269 (1994) 32411–32417.
[10] H. Yamada, T. Abe, A. Satoh, et al., Stabilization of actin bundles by a dynamin 1/cortactin ring complex is necessary for growth cone filopodia, J. Neurosci. 33 (2013) 4514–4526.
[11] E.S. Gold, D.M. Underhill, N.S. Morrissette, et al., Dynamin 2 is required for phagocytosis in macrophages, J. Exp. Med. 190 (1999) 1849–1856.
[12] A. Otsuka, T. Abe, M. Watanabe, et al., Dynamin 2 is required for actin assembly in phagocytosis in Sertoli cells, Biochem. Biophys. Res. Commun. 378 (2009) 478–482.
[13] K. Faelber, Y. Posor, S. Gao, et al., Crystal structure of nucleotide-free dynamin, Nature 477 (2011) 556–560.
[14] M.G. Ford, S. Jenni, J. Nunnari, The crystal structure of dynamin, Nature 477 (2011) 561–566.
[15] H. Damke, T. Baba, D.E. Warnock, et al., Induction of mutant dynamin specifically blocks endocytic coated vesicle formation, J. Cell Biol. 127 (1994) 915–934.
[16] D.A. Schafer, S.A. Weed, D. Binns, et al., Dynamin2 and cortactin regulate actin assembly and filament organization, Curr. Biol. 12 (2002) 1852–1857.
[17] O.L. Mooren, T.I. Kotova, A.J. Moore, et al., Dynamin2 GTPase and cortactin remodel actin filaments, J. Biol. Chem. 284 (2009) 23995–24005.
[18] C.B. Harper, M.R. Popoff, A. McCluskey, et al., Targeting membrane trafficking in infection prophylaxis: dynamin inhibitors, Trends Cell Biol. 23 (2013) 90–101.
[19] E. Macia, M. Ehrlich, R. Massol, et al., Dynasore, a cell-permeable inhibitor of dynamin, Dev. Cell 10 (2006) 839–850.
[20] H. Yamada, T. Abe, S.A. Li, et al., Dynasore, a dynamin inhibitor, suppresses lamellipodia formation and cancer cell invasion by destabilizing actin filaments, Biochem. Biophys. Res. Commun. 390 (2009) 1142–1148.
[21] H. Yamada, E. Ohashi, T. Abe, et al., Amphiphysin 1 is important for actin polymerization during phagocytosis, Mol. Biol. Cell 18 (2007) 4669–4680.
[22] H. Yamada, S. Padilla-Parra, S.J. Park, et al., Dynamic interaction of amphiphysin with N-wasp regulates actin assembly, J. Biol. Chem. 284 (2009) 34244–34256.
[23] R.D. Eppinga, E.W. Krueger, S.G. Weller, et al., Increased expression of the large GTPase dynamin 2 potentiates metastatic migration and invasion of pancreatic ductal carcinoma, Oncogene 31 (2012) 1228–1241.
[24] K. Edamura, Y. Nasu, M. Takaishi, et al., Adenovirus-mediated REIC/Dkk-3 gene transfer inhibits tumor growth and metastasis in an orthotopic prostate cancer model, Cancer Gene Ther. 14 (2007) 765–772.
[25] F. Soulet, D. Yarar, M. Leonard, et al., SNX9 regulates dynamin assembly and is required for efficient clathrin-mediated endocytosis, Mol. Biol. Cell. 16 (2005) 2058–2067.
[26] J. Zheng, S.M. Cahill, M.A. Lemmon, D. Fushman, J. Schlessinger, D. Cowburn, Identification of the binding site for acidic phospholipids on the pH domain of dynamin: implications for stimulation of GTPase activity, J. Mol. Biol. 255 (1996) 14–21.
[27] H.C. Lin, B. Barylko, M. Achiriloaie, J.P. Albanesi, Phosphatidylinositol (4,5)-bisphosphate-dependent activation of dynamins I and II lacking the proline/arginine-rich domains, J. Biol. Chem. 272 (1997) 25999–26004.
[28] A. Quan, A.B. McGeachie, D.J. Keating, et al., Myristyl trimethyl ammonium bromide and octadecyl trimethyl ammonium bromide are surface-active small molecule dynamin inhibitors that block endocytosis mediated by dynamin I or dynamin II, Mol. Pharmacol. 72 (2007) 1425–1439.
[29] H. Feng, K.W. Liu, P. Guo, et al., Dynamin 2 mediates PDGFRα-SHP-2-promoted glioblastoma growth and invasion, Oncogene 31 (2012) 2691–2702.
[30] T. Hara, K. Honda, M. Shitashige, et al., Mass spectrometry analysis of the native protein complex containing actinin-4 in prostate cancer cells, Mol. Cell Proteomics 6 (2007) 479–491.
[31] R. Gareus, A. Di Nardo, V. Rybin, et al., Mouse profilin 2 regulates endocytosis and competes with SH3 ligand binding to dynamin 1, J. Biol. Chem. 281 (2006) 2803–2811.
[32] M.M. Kessels, A.E. Engqvist-Goldstein, D.G. Drubin, et al., Mammalian Abp1, a signal-responsive F-actin-binding protein, links the actin cytoskeleton to endocytosis via the GTPase dynamin, J. Cell Biol. 153 (2001) 351–366.
[33] C. Gu, S. Yaddanapudi, A. Weins, et al., Direct dynamin-actin interactions regulate the actin cytoskeleton, EMBO J. 29 (2010) 3593–3606.
[34] J. Chua, R. Rikhy, J. Lippincott-Schwartz, Dynamin 2 orchestrates the global actomyosin cytoskeleton for epithelial maintenance and apical constriction, Proc. Natl. Acad. Sci. USA 106 (2009) 20770–20775.
[35] M. Chircop, S. Perera, A. Mariana, et al., Inhibition of dynamin by dynole 34–2 induces cell death following cytokinesis failure in cancer cells, Mol. Cancer Ther. 10 (2011) 1553–1562.
[36] H.M. Thompson, A.R. Skop, U. Euteneuer, et al., The large GTPase dynamin associates with the spindle midzone and is required for cytokinesis, Curr. Biol. 12 (2002) 2111–2117.